Journal of the European Ceramic Society **6** (1990) 375–381

Structural Reliability Evaluation of Ceramic Components*

Jyunichi Hamanaka, Akihiko Suzuki & Keiichi Sakai

Ishikawajima-Harima Heavy Industries Co. Ltd, 3-1-15 Toyosu, Koto-ku, Tokyo 135, Japan

(Received 22 February 1990; accepted 22 June 1990)

Abstract

An analytical evaluation method for the effect of proof testing applied to ceramic components is proposed. Based on this method, the effectiveness of a proof test can be evaluated even if the loading pattern is different from that in a service condition.

Es wird eine analytische Untersuchungsmethode zur Auswirkung des Proof-Tests an keramischen Teilen vorgeschlagen. Auf Grund dieser Methode kann die Wirksamkeit eines Proof-Tests auch dann abgeschätzt werden, wenn die Verteilung der Last von den im Betrieb vorliegenden Bedingung abweicht.

On propose ici une méthode d'évaluation analytique visant à déterminer l'influence de l'essai de résistance réalisé sur des pièces céramiques. Cette méthode permet d'évaluer l'efficacité d'un essai de résistance même si le type de charge est différent de celui des conditions en fonctionnement.

1 Introduction

Structural ceramics usually maintain high strength at elevated temperature and have eminent resistance against erosion. In contrast, ductility and toughness of ceramics are relatively lower compared to those of metals.

Moreover, the critical values of strength data are scattered over a wide range. Thus a comprehensive approach[1] is necessary for the application of ceramics to structural components, that is, methods for strength evaluation, design and assurance must be developed simultaneously. The relationships of these methods are shown in Fig. 1.

2 Proof Testing of Ceramic Components

The following methods can be considered to assure the integrity and reliability of ceramic components:

(1) Proof testing.
(2) Fracture testing of small-sized samples of the components.
(3) Non-destructive inspection.
(4) Combination of the above-mentioned methods.

Among these methods, proof testing is most reliable to assure the integrity of ceramic manufactures. In this section, a newly proposed method to evaluate the effect of proof testing is examined.

2.1 Fast fracture strength after proof testing[2]

In the uniaxial stress state, the failure probability of a ceramic component which has endured the proof testing is given as

$$P_p(\sigma_N) = \begin{cases} \dfrac{P(\sigma_N) - P(\sigma_p)}{1 - P(\sigma_p)} & \sigma_N \geq \sigma_p \\ 0 & \sigma_N < \sigma_p \end{cases} \qquad (1)$$

where $P(\sigma)$ is the failure probability of the components before the proof testing, and σ_N and σ_p are the nominal stress and proof testing stress, respectively.

For evaluating the effect of proof testing in the multiaxial and nonuniform stress states, the following are assumed:

(1) Penny-shaped flaws are uniformly distributed in a ceramic component (Fig. 2).
(2) The flaw surface direction is randomly oriented.

* Presented at the Advanced Materials Science and Engineering Society '89 Conference, Tokyo. (Y. Matsuo and M. Sakai: co-chairmen), 16–17 March 1989.

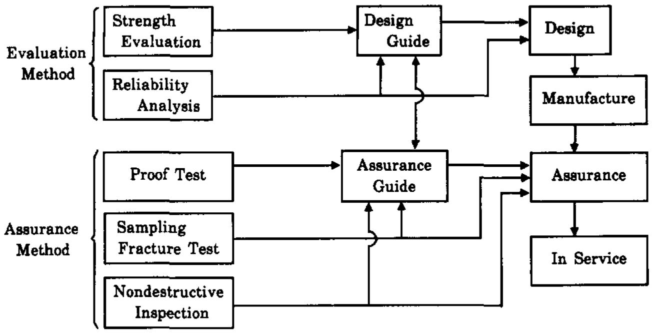

Fig. 1. Design and integrity assurance of ceramic components.

(3) The existence probability of a crack whose size is larger than a, $P(a)$, is expressed as

$$P(a) = 1 - \exp\left\{-\left(\frac{a_0}{a}\right)^{m/2} \cdot \frac{V}{V_0}\right\} \quad (2)$$

where a is the flaw size, m is the Weibull parameter and a_0 and V_0 are the reference flaw size and reference volume, respectively.

(4) Employing the energy release rate criterion for fracture rule, the equivalent normal stress Z is expressed as

$$Z = \{\sigma_n^2 + 4\tau_n^2/(2-\nu)^2\}^{1/2}$$

where σ_n and τ_n are the normal and shear stress acting on the flaw surface (Fig. 2).

2.1.1 Proof test whose loading pattern is similar to that for in service conditions

In the case of proof testing whose loading pattern is similar to that for in service conditions, the probability of fast fracture after proof testing can be obtained from eqn (1). Assuming that the strength distribution of fast fracture is given by a two-parameter Weibull distribution in uniaxial tension, $P(\sigma_N)$ in eqn (1) is represented as

$$P(\sigma_N) = 1 - \exp\left\{-\xi . \sigma_N^m . \int_V \int_0^{\pi/2} \int_0^{\pi/2} . \left(\frac{Z}{\sigma_N}\right)^m \times y(\sigma_n . 0) . \sin\phi . d\phi . d\theta . dv\right\} \quad (3)$$

where

$$\xi = \frac{1}{\Omega} . \Gamma\left(\frac{1}{m}+1\right)^m . \left(\frac{\sigma_N}{\bar{\sigma}_{ref}}\right)^m . \left(\frac{1}{V_{ref}}\right)$$

$$\Omega = \frac{2}{\pi} . \int_0^{\pi/2} \int_0^{\pi/2} \left\{\cos^4\phi + \frac{4}{(2-\nu)^2} \times (\cos^2\phi - \cos^4\phi)\right\}^{m/2} . \sin\phi \, d\phi \, d\theta$$

and σ_N is the nominal stress, $\bar{\sigma}_{ref}$ the average tensile strength using test specimen of volume V_{ref}, and $y(\sigma_n . 0)$ the Heaviside step function.

2.1.2 Proof test whose loading pattern is different from that in service condition

In the case of proof testing whose loading pattern is different from that in service conditions, eqn (1) is not applicable. So, a flaw in small element ΔV_i is considered, whose direction is oriented to the angle ϕ, θ as shown in Fig. 2. Then, the equivalent normal stress Z of such a flaw is constant in proof testing and in service condition. Namely, the failure probability of such a flaw which has endured proof testing can be expressed as

$$P_{p,\Delta ij}(\sigma_N) = \begin{cases} \dfrac{P_{\Delta ij}(\sigma_N) - P_{\Delta ij}(\sigma_p)}{1 - P_{\Delta ij}(\sigma_p)} & Z_{A,ij} \geq Z_{p,ij} \\ 0 & Z_{A,ij} < Z_{p,ij} \end{cases} \quad (4)$$

where subscript Δij means the value according to the flaw in ΔV_i, of which surface direction is oriented to the angle ϕ, θ. $Z_{A,ij}$ and $Z_{p,ij}$ are the equivalent normal stresses of the flaw in ΔV_i whose surface direction is oriented to the angle ϕ, θ under in service and proof testing conditions, respectively. $P_{\Delta ij}(\sigma_N)$ in eqn (4) is written as follows:

$$P_{\Delta ij}(\sigma_N) = 1 - \exp\left\{-\xi^* . Z_{A,ij}^m . y(\sigma_{nA} . 0) \times \sin\phi . \Delta\phi . \Delta\theta . \Delta V\right\} \quad \xi^* = \frac{\xi}{8}$$

Then the reliability of the above-mentioned flaw is given by

$$R_{p,\Delta ij}(\sigma_N) = \begin{cases} \dfrac{1 - P_{\Delta ij}(\sigma_N)}{1 - P_{\Delta ij}(\sigma_p)} & Z_{A,ij} \geq Z_{p,ij} \\ 1 & Z_{A,ij} < Z_{p,ij} \end{cases} \quad (5)$$

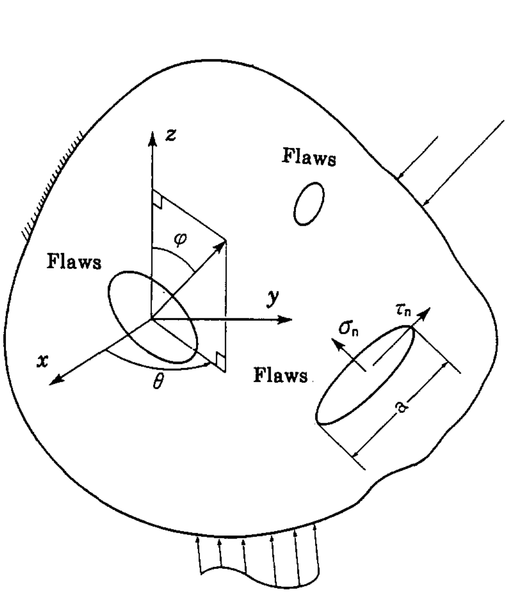

Fig. 2. Flaws in ceramic components.

By considering all flaws in ΔV_i, the reliability of the small element ΔV_i which has endured proof testing is obtained as

$$R_{p,\Delta i}(\sigma_N) = \prod_j R_{P,\Delta ij}(\sigma_N) = \frac{\prod_{Z_{A,ij} \geq Z_{P,ij}} \{1 - P_{\Delta ij}(\sigma_N)\}}{\prod_{Z_{A,ij} \geq Z_{P,ij}} \{1 - P_{\Delta ij}(\sigma_p)\}} \tag{6}$$

where

$$\prod_{Z_{A,ij} \geq Z_{P,ij}} \{1 - P_{\Delta ij}(\sigma_N)\}$$
$$= \prod_{\text{all } \phi,\theta} \exp\{-\xi^*.Z^m_{A,ij}y(\sigma_{nA}.0) \times y(Z_A - Z_p.0).\sin\phi\,\Delta\phi\,\Delta\theta\,.\Delta V\}$$
$$= \exp\left\{-\xi^*.\sum_{\text{all } \phi,\theta}.Z^m_{A,ij}.y(\sigma_{nA}.0) \times y(Z_A - Z_p.0).\sin\phi\,\Delta\phi\,\Delta\theta.\Delta V\right\}$$

Taking $\Delta\phi$, $\Delta\theta$ to be very small, the above equation can be expressed as follows:

$$\prod_{Z_{A,ij} \geq Z_{p,ij}} \{1 - P_{\Delta ij}(\sigma_N)\}$$
$$= \exp\left\{-\xi.\int_0^{\pi/2}\int_0^{\pi/2} Z^m_{A,i}y(\sigma_{nA}.0) \times y(Z_A - Z_p.0).\sin\phi\,d\phi\,d\theta.\Delta V\right\}$$

By substituting $Z_{p,i}$ and σ_{np} into $Z_{A,i}$ and σ_{nA} in the above equation, the denominator in eqn (6) can be obtained, where $Z_{p,i}$ and $Z_{A,i}$ are the equivalent normal stresses of Δi under proof testing and in service conditions, respectively.

Finally, by applying the weakest link theory to the component which is the assembly of the small element ΔV_i, the reliability of the ceramic components is given by

$$R_p(\sigma_N) = \prod_{\text{all } \Delta i} R_{p,\Delta i}(\sigma_N) = \frac{R_{p1}}{R_{p2}} \tag{7}$$

where

$$R_{P1} = \exp\left\{-\xi\int_V\int_0^{\pi/2}\int_0^{\pi/2} Z^m_A.y(\sigma_{nA}.0) \times y(Z_A - Z_P.0).\sin\phi.d\phi.d\theta.dv\right\}$$

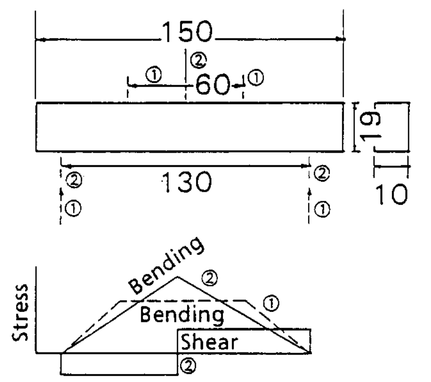

Fig. 3. Bending test specimen and loading pattern.

and

$$R_{P2} = \exp\left\{-\xi\int_V\int_0^{\pi/2}\int_0^{\pi/2} Z^m_p.y(\sigma_{nP}.0) \times y(Z_A - Z_P.0).\sin\phi.d\phi.d\theta.dv\right\}$$

Then, the failure probability of a component which has endured proof testing is obtained by subtracting $R_P(\sigma_N)$ from 1.

2.1.3 Fast fracture by bending test

For verification of the above-mentioned theory, bending tests were carried out using sintered Si_3N_4 test specimens. Proof test loading was applied by four point bending. The test specimens having endured this proof testing were fractured by three point bending.

Dimensions of the test specimen and loading patterns are shown in Fig. 3. The calculated and experimental results of the fracture strength after proof testing are shown in Fig. 4. These results show fairly good agreement.

2.2 Fatigue strength after proof testing[3]

2.2.1 Static fatigue strength after proof testing

The crack propagation rate under uniaxial stress state is assumed to be represented by

$$\frac{da}{dt} = BK_I^n \qquad K_I = C\sigma\sqrt{a} \tag{8}$$

where σ, a, C are applied stress, crack size parameter and the coefficient depending on the crack shape and loading pattern respectively. By integrating eqn (8), the static fatigue life t_f is obtained as

$$t_f = \zeta(\sigma).\left[\left\{\frac{1}{a_i}\right\}^{n-2/2} - \left\{\frac{1}{a_c(\sigma)}\right\}^{n-2/2}\right] \tag{9}$$

where a_i and $a_c(\sigma)$ are initial and critical flaw size respectively, and $\xi(\sigma)$ is

$$\zeta(\sigma) = \frac{2}{(n-2).B.C^n.\sigma^n} \tag{10}$$

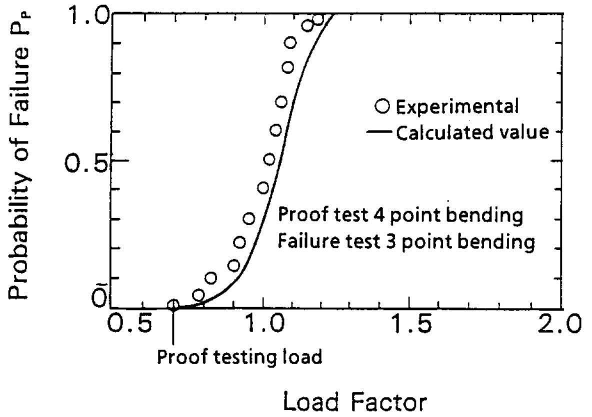

Fig. 4. Bending test results and calculated values.

When proof testing stress and applied stress are expressed as σ_p and σ_A, the minimum life t_p assured by proof testing is given by

$$t_p = \zeta(\sigma_A).\left[\left\{\frac{1}{a_p}\right\}^{n-2/2} - \left\{\frac{1}{a_c(\sigma_A)}\right\}^{n-2/2}\right] \quad (11)$$

where a_p is the maximum existing flaw size remaining after proof testing and is given by $K_{IC}^2/(C^2\sigma_p^2)$. In the uniaxial stress state, the static fatigue failure probability after proof testing is given by

$$P_p(t_f) = \begin{cases} \dfrac{P(t_f) - P(t_p)}{1 - P(t_p)} & t_f \geq t_p \\ 0 & t_f < t_p \end{cases} \quad (12)$$

If the proof test loading pattern is similar to that of the in service conditions, the static fatigue failure probability in multiaxial stress state can be expressed approximately as eqn (12). In this case, the minimum assured life t_p of a component in eqn (12) is calculated by

$$t_p = \zeta(Z_{A,max}).\left[\left\{\frac{1}{a_p}\right\}^{n-2/2} - \left\{\frac{1}{a_c}\right\}^{n-2/2}\right] \quad (13)$$

where $Z_{A,max}$, a_p and a_c are the maximum equivalent normal stress in the service condition, $K_{IC}^2/(C^2.Z_{p,max}^2)$ and $K_{IC}^2/(C^2.Z_{A,max}^2)$, respectively, and $P(t_f)$ in eqn (12) is represented as

$$P(t_f) = 1 - \exp\left\{-\xi.\int_V \int_0^{\pi/2} \int_0^{\pi/2} .(\eta.t_f.Z_A^n + Z_A^{n-2})^{m^*}.y(\sigma_{nA}.0)\sin\phi\, d\phi\, d\theta\, dv\right\} \quad (14)$$

where η and m^* are $(n-2).B.K_{IC}^{n-2}.C^2/2$ and $m/(n-2)$, respectively.

The effect of proof testing on static fatigue strength in the case where the loading pattern between proof testing and service condition are different may now be examined.

As discussed in Section 2.1.2, a flaw in the small element ΔV_i is considered, whose surface direction is oriented to the angle ϕ, θ, as shown in Fig. 2. The minimum life of this flaw assured by proof testing, t_{pij}, is given by

$$t_{pij} = \zeta(Z_{A,ij}).\left\{\left(\frac{1}{a_{pij}}\right)^{n-2/2} - \left(\frac{1}{a_{cij}}\right)^{n-2/2}\right\} \times y(\sigma_{np,ij}.0).y(Z_{p,ij} - Z_{A,ij}.0) \quad (15)$$

where $\sigma_{np,ij}$, a_{pij} and a_{cij} are the normal stress to the flaw surface under proof testing conditions, $K_{IC}^2/C^2(Z_{p,ij})^2$ and $K_{IC}^2/C^2(Z_{A,ij})^2$, respectively. Then, the static fatigue probability of this flaw which has endured proof testing is obtained as

$$P_{p,ij}(t_f) = \begin{cases} \dfrac{P_{ij}(t_f) - P_{ij}(t_{pij})}{1 - P_{ij}(t_{pij})} & t_f \geq t_{pij} \\ 0 & t_f < t_{pij} \end{cases} \quad (16)$$

where $P_{ij}(t_f)$ is

$$P_{ij}(t_f) = 1 - \exp\{-\xi^*.(\eta.t_f.Z_{A,ij}^n + Z_{A,ij}^{n-2})^{m^*}.y(\sigma_{nA}.0)\sin\phi\,\Delta\phi\,\Delta\theta\,\Delta V_i\} \quad (17)$$

$P_{ij}(t_{pij})$ is obtained by substituting t_{pij} into t_f in eqn (17). The reliability that this flaw does not fail within t_f is written as

$$R_{p,ij}(t_f) = \begin{cases} \dfrac{1 - P_{ij}(t_f)}{1 - P_{ij}(t_{pij})} & t_f \geq t_{pij} \\ 1 & t_f < t_{pij} \end{cases} \quad (18)$$

By considering all flaws in ΔV_i, the reliability of the small element ΔV_i which has endured proof testing is obtained as

$$R_{p,i}(t_f) = \frac{\prod_{t_f \geq t_{Pij}} \{1 - P_{ij}(t_f)\}}{\prod_{t_f \geq t_{Pij}} \{1 - P_{ij}(t_{pij})\}} \quad (19)$$

where

$$\prod_{t_f \geq t_{Pij}}$$

means that products for the limited number of flaws in a condition $t_{pij} \leq t_f$.

Using the Heaviside step function $y(t_f - t_{pij}.0)$, the numerator in eqn (19) is represented as

$$\prod_{t_f \geq t_{pij}} \{1 - P_{ij}(t_f)\} = \prod_{\text{all } \phi,\theta} \exp\{-\xi^*.(\eta.t_f.Z^n_{A,ij} + Z^{n-2}_{A,ij})^{m^*} \times y(\sigma_{nA}.0).y(t_f - t_{pij}.0) \times \sin\phi\,\Delta\phi\,\Delta\theta\,\Delta V_i\}$$

$$= \exp\left\{-\xi^* \sum_{\text{all } \phi,\theta} (\eta.t_f.Z^n_{A,ij} + Z^{n-2}_{A,ij})^{m^*} \times y(\sigma_{nA}.0).y(t_f - t_{pij}.0) \times \sin\phi\,\Delta\phi\,\Delta\theta.\Delta V_i\right\}$$

Taking $\Delta\phi$, $\Delta\theta$ to be very small, the above equation can be expressed as

$$\prod_{t_f \geq t_{pij}} \{1 - P_{ij}(t_f)\}$$

$$= \exp\left\{-\xi.\int_0^{\pi/2}\int_0^{\pi/2} (\eta.t_f.Z^n_{A,i} + Z^{n-2}_{A,ij})^{m^*} y(\sigma_{nA}.0).y(t_f - t_{pij}.0) \times \sin\phi\,d\phi\,d\theta.\Delta V_i\right\} \quad (20)$$

where $Z_{A,i}$ is the equivalent nominal stress of ΔV_i under service conditions. By substituting t_{pij} into t_f in eqn (20), the denominator in eqn (19) can be obtained. By applying the weakest link theory to the component itself, which is an assembly of small elements, the reliability of the component is

$$R_p(t \leq t_f) = \prod_{\text{all } \Delta i} R_{p,i}(t_f) = \frac{R_{P1}}{R_{P2}} \quad (21)$$

where R_{P1} and R_{P2} are represented as

$$R_{P1} = \exp\left\{-\xi\int_V\int_0^{\pi/2}\int_0^{\pi/2} (\eta.t_f.Z^n_A + Z^{n-2}_A)^{m^*} \times y(\sigma_{nA}.0).y(t_f - t_{pij}.0).\sin\phi\,d\phi\,d\theta.dv\right\}$$

$$R_{P2} = \exp\left\{-\xi\int_V\int_0^{\pi/2}\int_0^{\pi/2} (\eta.t_{pij}.Z^n_A + Z^{n-2}_A)^{m^*} \times y(\sigma_{nA}.0).y(t_f - t_{pij}.0).\sin\phi\,d\phi\,d\theta.dv\right\}$$

Then the failure probability of a component during the lifetime t_f is obtained as

$$P_p(t_f) = \begin{cases} 1 - R_p(t \leq t_f) & t_f \leq t^*_p \\ 0 & t_f > t^*_p \end{cases} \quad (22)$$

where t^*_p is the minimum value of t_{pij}.

2.2.2 Reliability analysis of turbine disk

In order to verify the above-mentioned theory, reliability analysis of a gas turbine disk was performed. The analysis model of the gas turbine disk is shown in Fig. 5. The heat transfer condition is shown in the same figure. Centrifugal force and thermal loading due to gas flow are applied to the disk. The disk material is hot-pressed silicon nitride, and its thermal conductivity, specific heat, and specific gravity are 19 W/(m.K), 0·92 kJ/(kg.K) and $3{\cdot}26 \times 10^3$ kg/m^3, respectively. Young's modulus, Poisson's ratio, and linear expansion are 3×10^5 MPa, 0·27 and $3{\cdot}7 \times 10^{-6}$/°C, respectively. For the Weibull parameter, σ_{ref}, V_{ref} and K_{IC}, values of

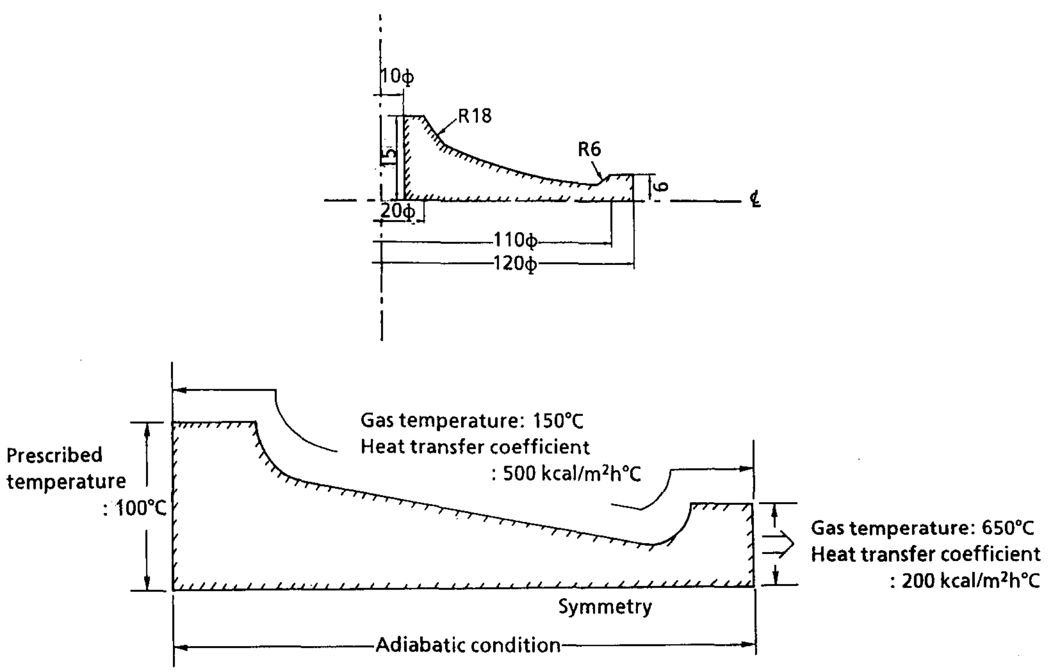

Fig. 5. Analysis model of gas turbine disk.

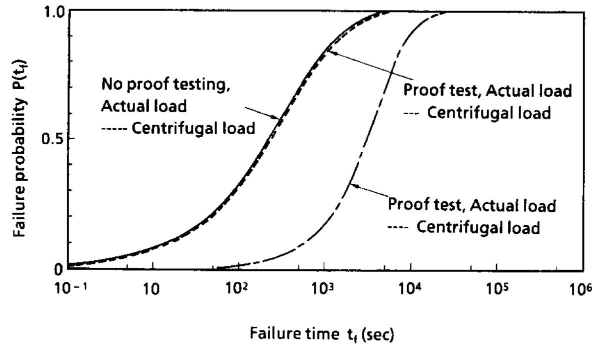

Fig. 6. Failure probability of turbine disk due to centrifugal loading.

9·0, 760 MPa, 8600 mm^3 and 3·1 MPa.m$^{1/2}$ respectively are used. Values of C, B and n in eqn (8) are 1·13, 2·8 × $10^{-1\cdot 3}$ m/s (MPa.m$^{1/2}$)$^{-n}$ and 15, respectively. The rotating speed under service conditions is 30 000 rpm. Calculated results of the failure probability due to centrifugal force are shown in Fig. 6.

In this figure, the solid line is the calculated result for the rotating speed of 30 000 rpm without proof testing. The dotted and chained lines are calculated results in the case where the disk endured 50 000 rpm proof testing. The dotted line is for results calculated from eqns (12) and (14). The chained line is for results calculated from eqn (22). Equation (12) can be used for this example, because the loading pattern of proof testing is similar to that for in-service conditions. But the effect of proof testing can not be seen in the results expressed by the dotted line. This is explained by the fact that t_p in eqn (12) is so small ($\simeq$0·02 s) that $P(t_p)$ in eqn (12) is almost zero and $P_p(t_f)$ is almost $P(t_f)$. In the analysis of the chained line, the minimum assured life t_{pij} is determined for every element and every flaw. So, the effect of proof testing can be seen in the results expressed by the chained line.

Calculated results of the failure probability due to centrifugal force and thermal loading are shown in Fig. 7. In this figure, the failure probability without

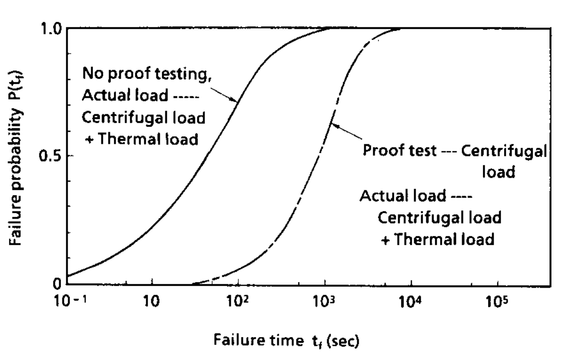

Fig. 7. Failure probability of turbine disk due to centrifugal and thermal loadings.

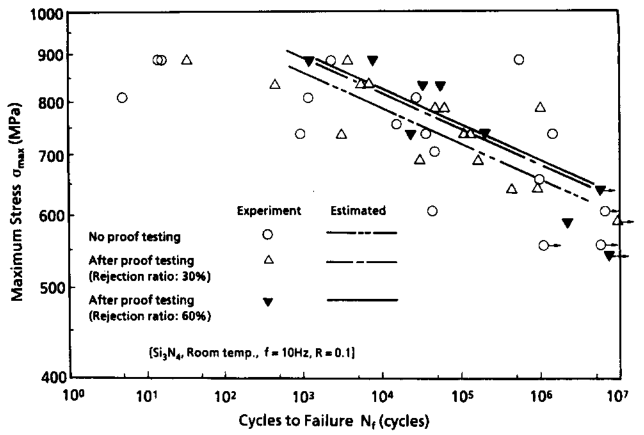

Fig. 8. Cyclic fatigue strength after proof testing.

proof testing is expressed by the solid line and that with 50 000 rpm proof testing is expressed by the chained line. Figure 7 shows that the static fatigue life of a gas turbine disk can be extended by proof testing whose loading pattern is different from that in service condition.

2.2.3 Cyclic fatigue strength after proof testing

As the mechanism of cyclic fatigue fracture, the following two types of fracture can be considered:

(1) Time-dependent fracture.
(2) Cyclic-dependent fracture.

The time-dependent fracture in cyclic fatigue can be evaluated by slow crack growth under a varying load. Then the effect of proof testing can be evaluated by applying the above-mentioned theory about static fatigue. In the case of cyclic-dependent fracture, it can be considered that the fatigue fracture is caused by cyclic dependent crack growth from the initial flaws.

The crack growth rate is assumed as follows:

$$\frac{da}{dN} = B\{K_{\max}(1 - aR)\}^n \tag{23}$$

where K_{max} and R are maximum stress intensity factor and stress ratio, respectively. Then the effect of proof testing can be evaluated by replacing t_f, $P(t_f)$, $P_p(t_f)$, t_{pij}, B, $Z_{A,ij}$ in eqns (12) and (22) by N_f, $P(N_f)$, $P_p(N_f)$, N_{pij}, $B(1 - aR)^n$ and $(Z_{A,ij})_{max}$, respectively. Test results by four point bending are shown in Fig. 8 with the average life estimated by the above-mentioned theory. Agreement between the test results and calculated results is observed.

3 Conclusion

Assurance methods for structural ceramic components are discussed. A new evaluation method for the effect of the proof testing is proposed in the case where the loading pattern is different from that for in-service conditions.

Acknowledgement

A part of this work was performed under the contract between the Agency of Industrial Science and Technology of MITI and the Engineering Research Association for High Performance Ceramics, as a part of R&D Project of Basic Technology for Future Industries.

References

1. Suzuki, A., *et al.*, *Trans JSME, A*, **53**-495 (1987) 2134.
2. Hamanaka, J., *et al.*, *Trans JSME, A*, **53**-492 (1987) 1638.
3. Hamanaka, J., *et al.*, *Trans JSME, A*, to be submitted.